

Electronic Supplementary Information

Ultrasensitive electrochemical immunoassay for melanoma cells using mesoporous polyaniline

M.U. Anu Prathap^a, Carlos Iván Rodríguez^b, Omer Sadak^c, Jiehao Guan^a, Vijaysaradhi Setaluri^{b*},
and Sundaram Gunasekaran^{a,c*}

^a*Department of Biological Systems Engineering, University of Wisconsin–Madison, 460 H Mall, Madison, WI 53706, USA.*

^b*Department of Dermatology, School of Medicine and Public Health, University of Wisconsin–Madison, 1300 University Avenue, B-25, Madison, WI 53706, USA.*

^c*Department of Materials Science and Engineering, University of Wisconsin–Madison, 1509 University Avenue, Madison, WI 53706, USA.*

**Electronic mail: vsetaluri@dermatology.wisc.edu (V. Setaluri), guna@wisc.edu (S. Gunasekaran)*

Part I: Experimental Details

Materials: All chemicals were used as received without further purification. Anti-MC1R antibodies (200 µg/mL) were obtained from Santa Cruz Biotechnology Inc. (Santa Cruz, CA). Nafion (0.5 wt%), carbonyldiimidazole, bovine serum albumin, HCl (37%), aniline, and ammonium persulphate (APS) were purchased from Sigma-Aldrich and Alfa Aesar. Deionized water from Millipore Milli-Q system (Resistivity 18.2 MΩ cm) was used in the electrochemical studies.

Synthesis of Polyaniline nanofibers: Polyaniline (PANI) nanofibers were synthesized through a modified interfacial polymerization method on the interface of two immiscible solvents (chloroform/water).¹ In a typical synthesis, 50 μL of aniline was dissolved in 5 mL chloroform (CHCl_3) which was designed as the organic phase, and 50 mmol ammonium persulphate (APS) was dissolved in 2.5 mL hydrochloric acid (1 mol L^{-1}) which was designed as the water phase. Then the above two solutions were transferred to a glass vial, generating an interface between the organic phase and water phase. During the reaction time, the green product slowly forms at the interface (Fig. S1). Polymerization was carried under static conditions for 20 h at 5 $^\circ\text{C}$. The resulting dark-green precipitate was filtered and rinsed with deionized water and ethanol for several times for removing excess acid and finally dried at 70 $^\circ\text{C}$ for 8 h.

Material characterizations: X-ray diffraction (XRD) analysis was investigated using X-ray diffractometer (PANalytical X'PERT PRO, using CuK-alpha radiation, $\lambda=0.1542 \text{ nm}$, 40 kV, 20 mA). Scanning Electron Microscopy (FESEM, LEO 1530-1) and Transmission electron microscopy (TEM, Tecnai-TF30) operated at 300 kV was used to observe the morphological characteristics. N_2 adsorption studies were performed on the Autosorb-IQ Quantachrome Instruments at 77 K. The sample was degassed at 423 K under vacuum before the measurements. The X-ray photoelectron spectroscopy (XPS) was employed in an XPS spectrometer to analyze the surface chemical composition and elemental distribution of polyaniline (Thermo Scientific K Alpha instrument). The current-voltage measurements were carried out by using Hewlett-Packard 4142B Modular DC source/monitor connected to an HP 34401A multimeter with a contact four-point probe station (Cascade Microtech Inc., Beaverton, Oregon, USA). UV-visible spectra were recorded on Lambda 25, PerkinElmer spectrometer in the wavelength range of 200–1100 nm. FTIR spectroscopic tests were conducted on FTIR Bruker TENSOR-27.

Electrochemical measurements: Electrochemical experiments were performed using CHI-660D electrochemical workstation (CHI Instruments Inc., USA) using disposable screen-printed electrode (SPE), the electrode pattern includes 3-mm diameter carbon working electrode, carbon counter electrode, and silver/silver chloride reference electrode. Screen-printed electrodes (SPE) were purchased from Zensor Research & Development Company Limited (Texas, USA). All

Electrochemical studies were carried out in the presence of 5 mM $K_3[Fe(CN)_6]/K_4[Fe(CN)_6]$ (1:1) solution in 0.1 M KCl (pH 7). The resultant Nyquist plots from EIS were analyzed using an equivalent circuit model available in Z-view software (Scribner Associates Inc., Pines, NC, USA).

Fabrication of the polyaniline immunosensor: Catalyst ink was prepared by mixing 5.0 mg of the prepared polyaniline catalyst with a mixture of 100 μ L Nafion (0.5 wt%) and 0.9 mL of water, after that dispersed by sonication for 1 h to obtain a well-dispersed suspension. Then, 2 μ L catalyst ink (Polyaniline nanofibers) was drop-casted onto the SPE working surface of the electrode and left to air dry for 3 h, leaving the material mounted onto the SPE surface. For antibody-MC1R functionalization onto polyaniline modified electrode surface, first, the modified electrode was activated with the 0.5 M carbonyldiimidazole (CDI) for 3 h at room temperature, which helps to increase the amount of MC1R antibody loading. 1 μ L (200 ng) aliquot of MC1R-Ab (200 μ g/mL) was then immobilized on the activated polyaniline modified electrode surface and incubated overnight at 4 °C. Lastly, the electrode was treated with a solution of bovine serum albumin (BSA, 0.5%) for 15 min to block nonspecific sites on the electrode. This electrode was carefully rinsed three times with phosphate buffer (pH=7.2). The immunosensor fabrication is presented in [Scheme 1](#).

Cell line and cell culture: Electrochemical experiments were performed using Melanoma (SK-MEL-2) and non-melanoma (human embryonic kidney (HEK)-293) cell lines (American Type Culture Collection (Manassas, VA)). Cell culture was under standard tissue culture conditions based on the standard procedure at 37 °C in a 5% CO₂ humidified atmosphere.² Cells were allowed to grow after which they were dislodged by using 0.25% Trypsin–EDTA (Life Technologies, GrandIsland, NY), or 2% EDTA solution in 1 x PBS (Sigma, St.Louis, MO), or a cell scraper (Sarstedt, Newton, NC). The number of cells (total and non-viable) was determined by the Trypan Blue dye method using a hemocytometer. The optical micrograph of the cell suspension is shown in [Fig. S8](#). The cell suspension was centrifuged at 1000 rpm for 2 min at 4 °C and the cell pellet was suspended in sterile PBS (pH=7.2) for further analysis.

Part II: Supplementary Figures

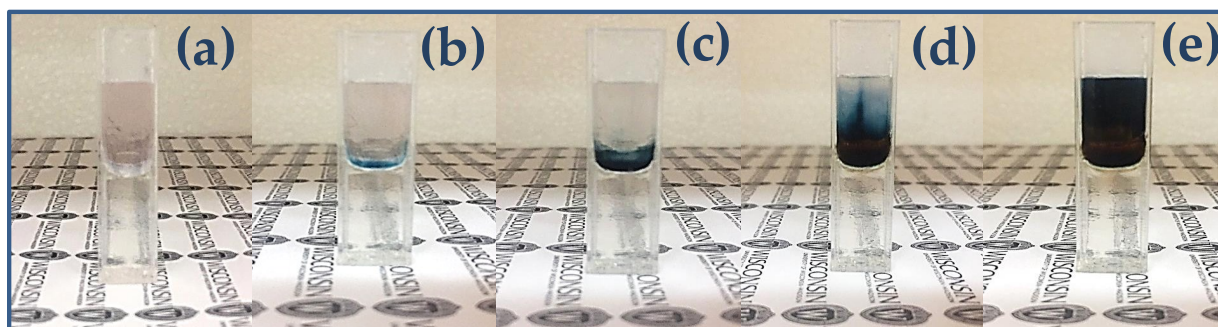


Figure S1 Snapshots showing the interfacial polymerization of aniline at reaction times of (a) 0, (b) 2, (c) 5, (d) 10, and (e) 120 min. The upper aqueous phase is ammonium persulphate dissolved in aqueous solution of hydrochloric acid and the bottom organic phase is aniline dissolved in chloroform.

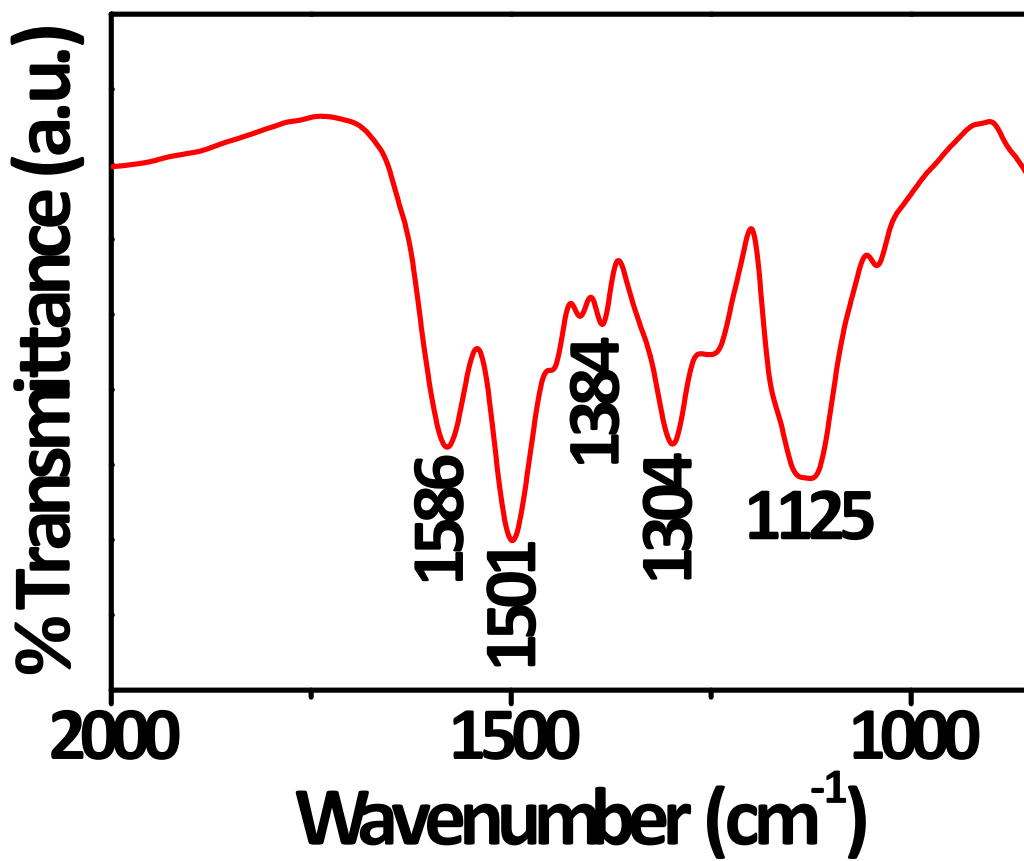


Figure S2 FT-IR spectra of PANI synthesized for this study.

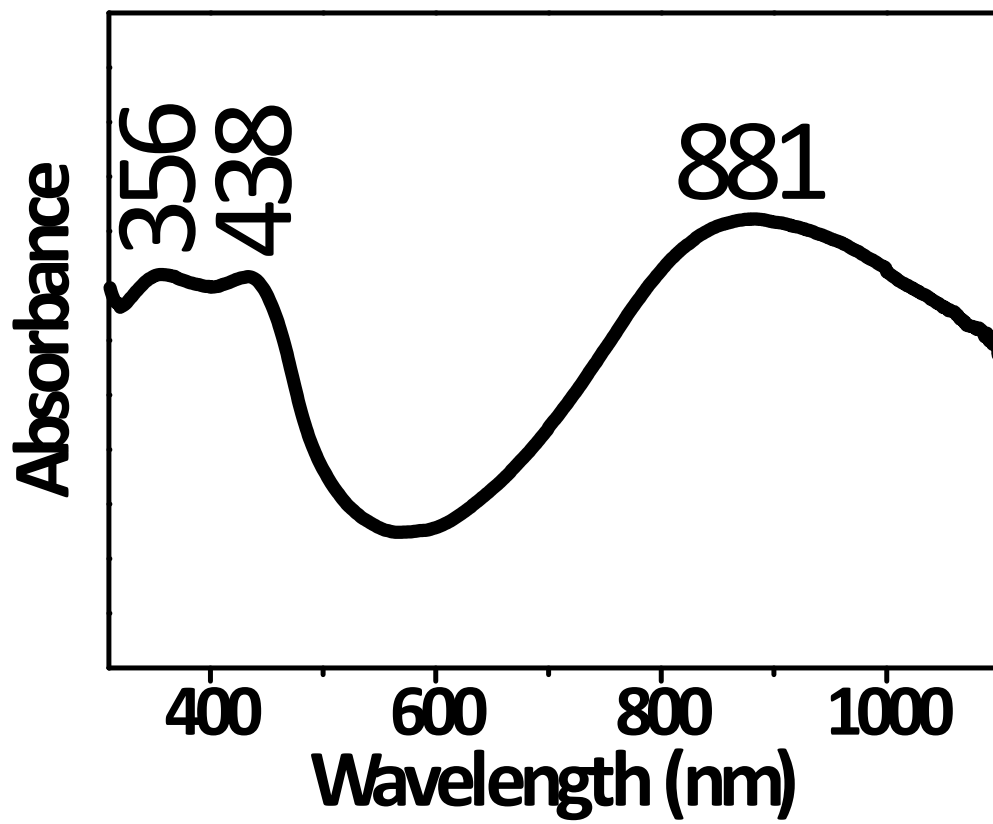


Figure S3 UV-visible spectra of PANI sample.

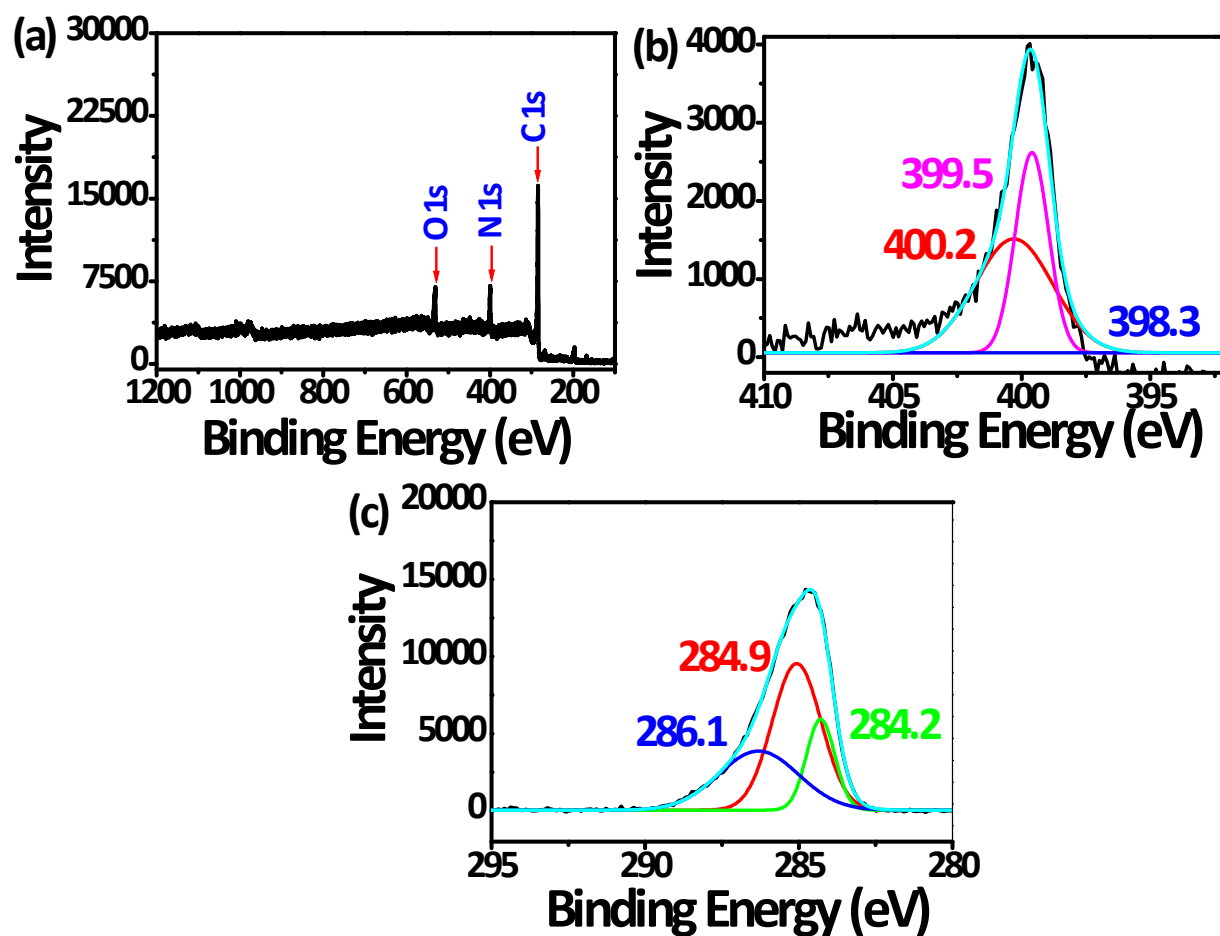


Figure S4. XPS spectra of PANI (a) survey spectrum and high-resolution spectra for (b) N 1s, and (c) C 1s.

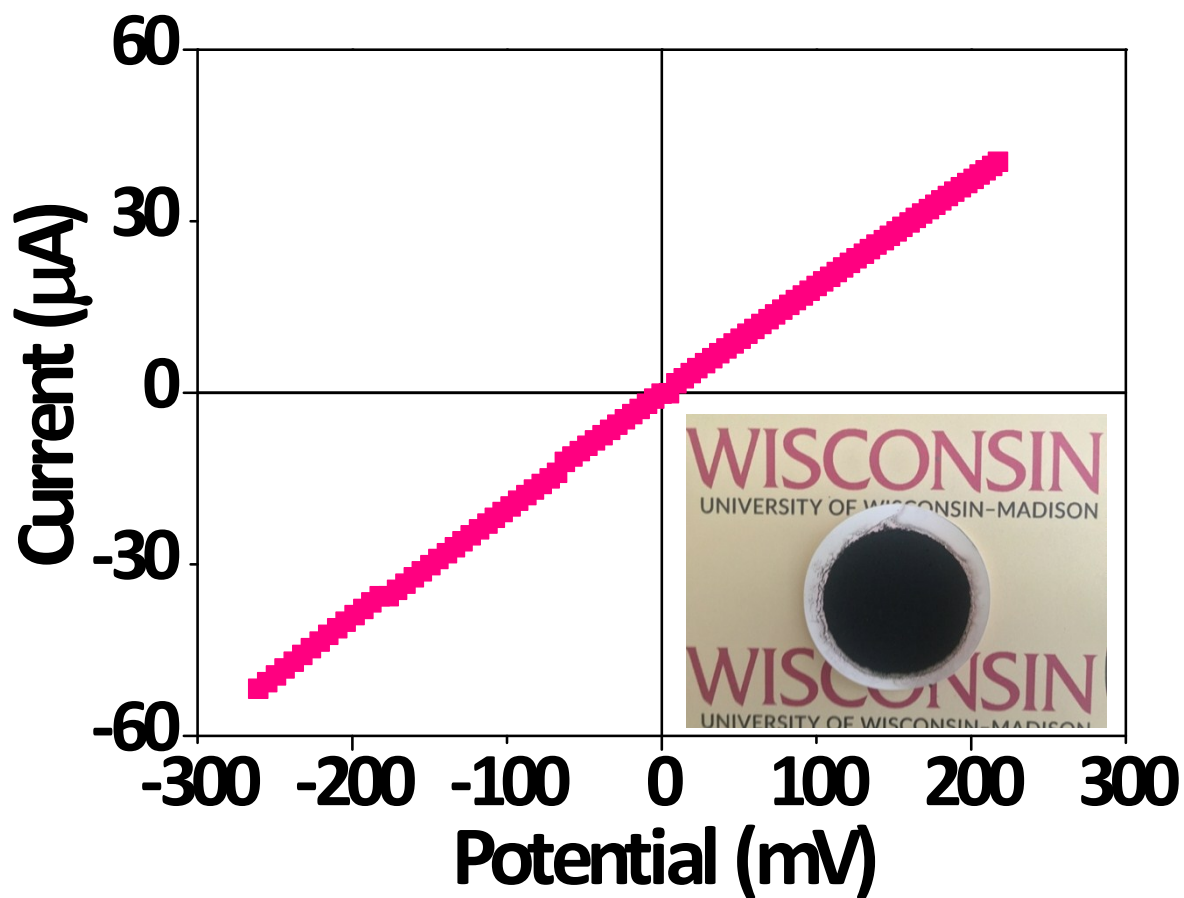


Figure S5. I-V curve of polyaniline at room temperature. The inset is a picture of PANI filtration film used for measurement.

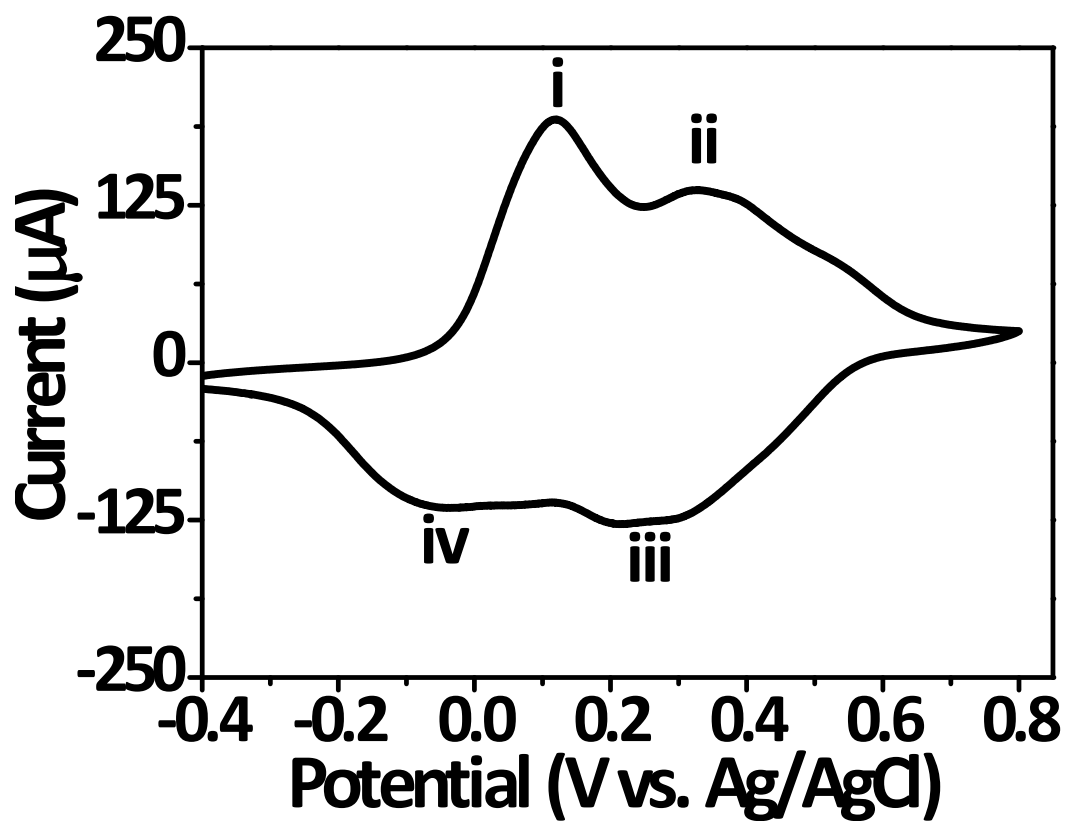


Figure S6 CV curve of PANI film at a scan rate of 50 mV/s in 1.0 mol/L H₂SO₄. The first pair of redox peaks (denoted as i/iv) corresponds to the interconversion of leucoemeraldine (LE) to emeraldine base (EB). The second pair of redox peaks (denoted as ii/iii) is due to oxidation of emeraldine base to oxidized pernigraniline (PN) and vice-versa.

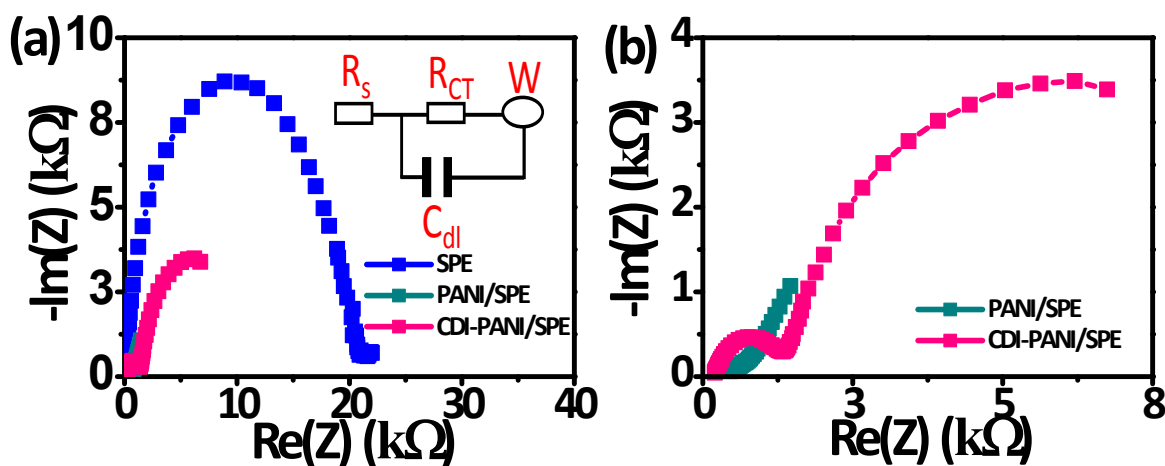


Figure S7 (a) Nyquist diagrams for SPE, PANI/SPE, and CDI-PANI/SPE recorded in the frequency range of 0.1 Hz to 10 kHz at a standard potential of +0.15 V (E_{app}), using a sinusoidal potential perturbation with an amplitude of 5 mV in 0.1 M KCl solution containing 5 mM $[\text{Fe}(\text{CN})_6]^{3-/4-}$. Inset circuit model used to fit the EIS spectra. (b) Details of (a) at low impedance for CDI-PANI/SPE and with for PANI/SPE. R_s : solution resistance, R_{CT} : charge-transfer resistance, C_{dl} : double layer capacitance, W : Warburg impedance.

Table S1. EIS characteristic parameters at various stages of surface modifications of the electrode.

Electrode	R_{CT} (Ω)	C_{dl} (F)	W ($\Omega \text{ cm}^2$)
SPE	19070	1.02×10^{-7}	0.35×10^{-3}
PANI	241.3	2.69×10^{-7}	0.78×10^{-3}
PANI/CDI	707.2	1.093×10^{-6}	0.2×10^{-3}

Table S2. EIS parameters of the MC1R-Ab-PANI/SPE on immunoreaction with different concentration of SKMEL-2 cells.

Sample	R_s (Ω)	CPE_{AB} [μF]	CPE_{CELL} [μF]	C_E [μF]	R_{AB} [Ω]
MC1R-Ab-PANI/SPE	284.3	171	-	4.6	1053
MC1R-Ab-PANI/SPE (SKMEL-2 1000 cells)	275.2	192	144	6.5	1357
MC1R-Ab-PANI/SPE (SKMEL-2 5000 cells)	274.2	381	98	9.1	1679

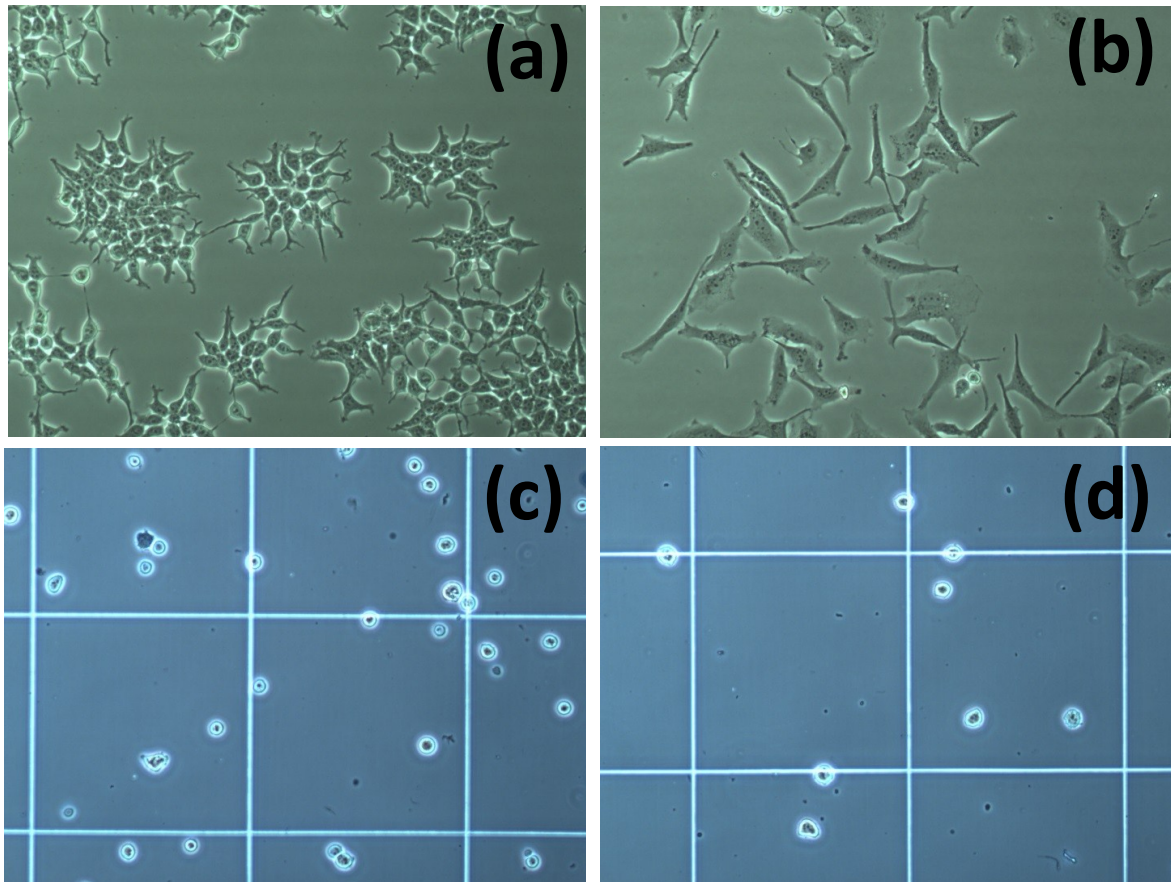


Figure S8 Typical micrographs of (a) HEK 293 and (b) SKMEL-2 cells and as viewed through microscope after trypsinization (stained with trypan blue) of (c) HEK 293 and (d) SKMEL-2 cells.

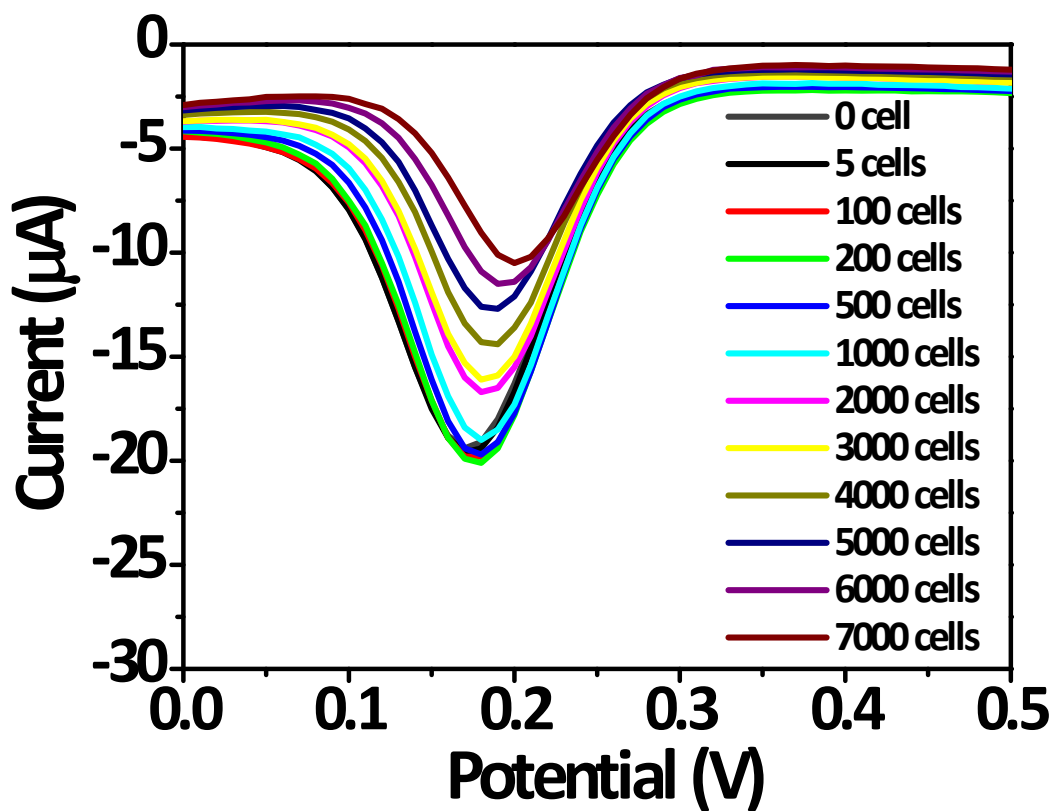


Figure S9 DPV curves obtained with different SKMEL-2 cells densities from 0 to 7000 cells/5 mL at MC1R-Ab-PANI/SPE (antibody loading 100 ng).

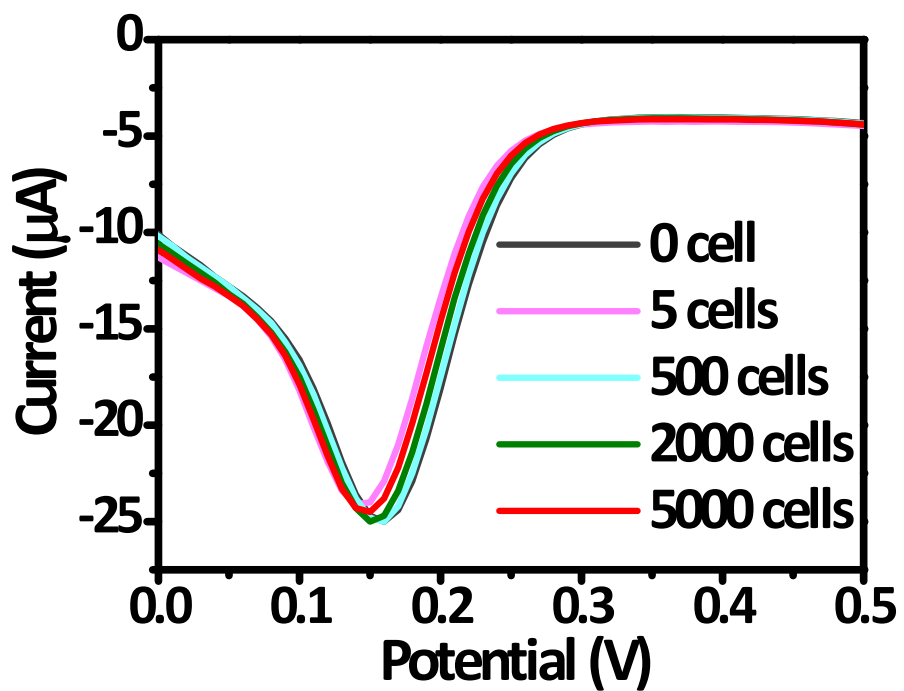


Figure S10 (a) DPV curves with different HEK293 cell densities from 0 to 5000 cells/5 mL at MC1R-Ab-PANI/SPE (antibody loading 200 ng).

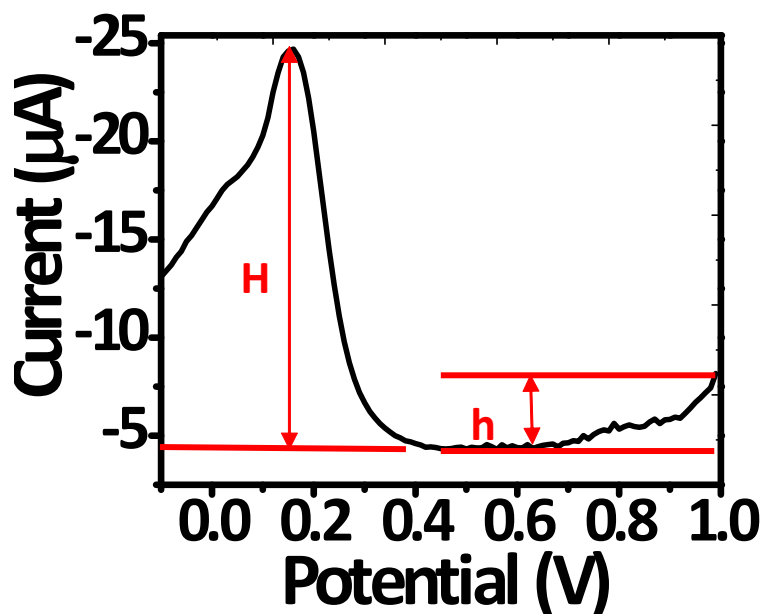


Figure S11 DPV curve for SKMEL-2 cells (5 cells/5mL) at MC1R-Ab-PANI/SPE (Simulation of an experimental response using the method of EP).

The signal-to-noise ratio is calculated from Equation (1).

$$S/N=2H..... \text{Eq. 1.}$$

Where, H is the height of the peak, and h is the peak-to-peak background noise.

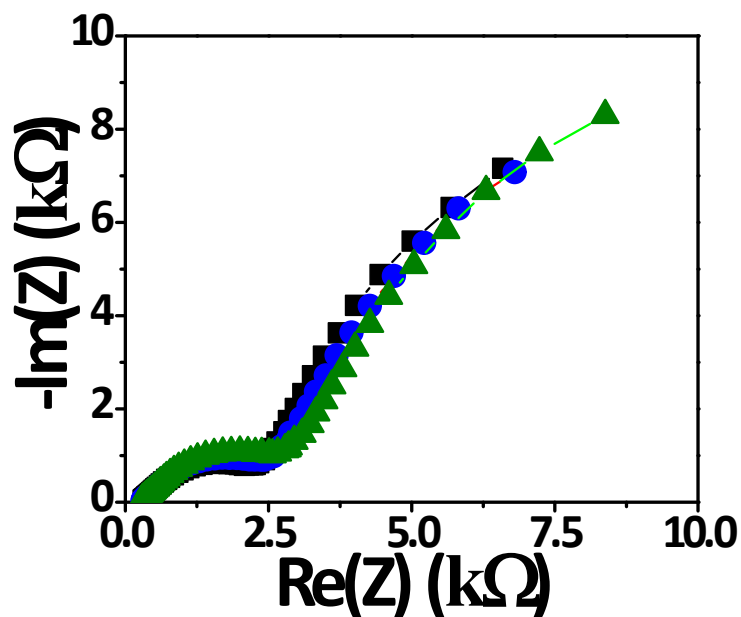


Figure S12 EIS of samples spiked with 400 SKMEL-2 cells at three-day intervals over nine days at MC1R-Ab-PANI/SPE in 5 mM $[\text{Fe}(\text{CN})_6]^{3-/4-}$ and 0.1 M KCl as the redox probe recorded in the frequency range of 0.1 Hz to 10 kHz at a standard potential of +0.15 V (E_{app}), using a sinusoidal potential perturbation with an amplitude of 5 mV.

Table S3. Comparison of previously reported electrochemical immunosensors for detecting cancer cells with the present work.

Procedure	Cell line	Incubation time (min)	Technique	Linear range (cells/mL)	LOD/LOQ (cells/mL)	Reference
Carbon Nanofiber-Doped Chitosan	K562	120	EIS	5.0×10^3 – 5.0×10^7	1000	3
RGDS/TA/Au/ITO	HeLa	60	DPV	3.0×10^2 – 1.0×10^7	300	4
CNTs@PDA-FA	HeLa	50	EIS	5.0×10^3 – 5.0×10^6	500	5
GE/AuNPs/MUA/FA	HeLa	–	EIS	6.0 – 1.0×10^3 and 1.0×10^3 – 1.0×10^6	6	6
Au/MPA/(Fc- PEI/SWNT)5/FA	HeLa	30	DPV	10 – 1.0×10^6	10	7
anti-CD146 coated-PN-nanovelcro chip	M229 (melanoma)	–	laser micro-dissection	–	36, 43 and 45	8
anti-EpCAM-gold array electrode	DU145 human prostate cancer	15	DPV	–	125	9
Peptide nanotube folic acid modified graphene	HeLa	10	CV	250 – 5000	250	10
MC1R-Ab/n-SiNPs/PPy/SPE	SKMEL-2 & WM-35 (melanoma)	15	CV	50–7500/2.5 mL	20	11
GE/BSA incorporated Ag nanoflowers/GA/SNA	DLD-1	120	EIS	1.35×10^2 – 1.35×10^7	40	12
GE/Au@BSA/GA/anti-CEA	BXPC-3	240	EIS	52 – 5.2×10^7	18	13
GCE/Poly-Llysine	T cell	-	Fluorescence	500 – 5.2×10^5	180	14
GCE/MWNT/AuNP/SA	A549	50	DPV	3.0×10^4 – 3.0×10^7	700	15
GE/Ag@BSA	KB	120	DPV	60 – 1.2×10^8	20	16
GE/PPy-Ag@BSA/PDITC/APBA	786-O	60	EIS	17 – 1.7×10^6	6	17
Cellulose/SWNT/Au	K562	120	EIS	1.6×10^4 – 1.0×10^7	2600	18
Nano-TiO ₂ /ITO electrode	K562/ADM	120	EIS	1.6×10^4 to 1.0×10^7	1300	19

PS@PANI/Au composites	HL-60 leukemia	120	EIS	1.6×10^3 to 1.6×10^8	730	²⁰
Polyaniline nanofibers/MCIR-Ab (MC1R-Ab-PANI/SPE)	SKMEL-2 (melanoma)	15	DPV	15-7000 cells/5mL	1 (LOQ)	Present Work
<p>Arg-Gly-Asp-Ser tetrapeptide (RGDS), Thiocctic acid (TA), Indium tin oxide (ITO), carbon nanotubes (CNT), polydopamine (PDA), folic acid (FA), 11-mercaptopundecanoic acid (MUA), poly(ethylene imine) functionalized with ferrocene (Fc-PEI), single-wall carbon nanotubes (SWNTs), multiwalled carbon nanotubes (MWNT) 3-mercaptopropionic acid (MPA), poly(lactic-co-glycolic acid)-nanofiber (PN), amino functionalized silica nanoparticles(n-SiNPs), bovine serum albumin (BSA), polypyrrole (PPy), screen printed electrode(SPE), glassy carbon electrode (GCE), electrochemical impedance spectroscopy (EIS), differential pulse voltammetry (DPV), cyclic voltammetry (CV).</p>						

Notes and references

- 1 J. Huang and R. B. Kaner, *Angew. Chemie - Int. Ed.*, 2004, **43**, 5817–5821.
- 2 N. Maddodi, W. Huang, T. Havighurst, K. Kim, B. J. Longley and V. Setaluri, *J. Invest. Dermatol.*, 2010, **130**, 1657–1667.
- 3 C. Hao, L. Ding, X. Zhang and H. Ju, *Anal. Chem.*, 2007, **79**, 4442–4447.
- 4 X. Wang, J. Ju, J. Li, J. Li, Q. Qian, C. Mao and J. Shen, *Electrochim. Acta*, 2014, **123**, 511–517.
- 5 T.-T. Zheng, R. Zhang, L. Zou and J.-J. Zhu, *Analyst*, 2012, **137**, 1316–1318.
- 6 R. Wang, J. Di, J. Ma and Z. Ma, *Electrochim. Acta*, 2012, **61**, 179–184.
- 7 J. Liu, Y. Qin, D. Li, T. Wang, Y. Liu, J. Wang and E. Wang, *Biosens. Bioelectron.*, 2013, **41**, 436–441.
- 8 S. Hou, L. Zhao, Q. Shen, J. Yu, C. Ng, X. Kong, D. Wu, M. Song, X. Shi, X. Xu, W. H. Ouyang, R. He, X. Z. Zhao, T. Lee, F. C. Brunnicardi, M. A. Garcia, A. Ribas, R. S. Lo and H. R. Tseng, *Angew. Chemie - Int. Ed.*, 2013, **52**, 3379–3383.
- 9 M. Moscovici, A. Bhimji and S. O. Kelley, *Lab Chip*, 2013, **13**, 940.
- 10 J. J. Castillo, W. E. Svendsen, N. Rozlosnik, P. Escobar, F. Martínez and J. Castillo-León, *Analyst*, 2013, **138**, 1026–31.
- 11 R. Seenivasan, N. Maddodi, V. Setaluri and S. Gunasekaran, *Biosens. Bioelectron.*, 2015, **68**, 508–515.
- 12 H. Cao, D. P. Yang, D. Ye, X. Zhang, X. Fang, S. Zhang, B. Liu and J. Kong, *Biosens. Bioelectron.*, 2015, **68**, 329–335.
- 13 C. Hu, D. P. Yang, Z. Wang, P. Huang, X. Wang, D. Chen, D. Cui, M. Yang and N. Jia, *Biosens. Bioelectron.*, 2013, **41**, 656–662.
- 14 L. L. Huang, Y. J. Jin, D. Zhao, C. Yu, J. Hao and H. Y. Xie, *Anal. Bioanal. Chem.*, 2014, **406**, 2687–2693.
- 15 X. Zhang, Y. Teng, Y. Fu, L. Xu, S. Zhang, B. He, C. Wang and W. Zhang, *Anal. Chem.*, 2010, **82**, 9455–9460.
- 16 C. Hu, D. P. Yang, K. Xu, H. Cao, B. Wu, D. Cui and N. Jia, *Anal. Chem.*, 2012, **84**, 10324–10331.
- 17 L. Zhang, C. Yu, R. Gao, Y. Niu, Y. Li, J. Chen and J. He, *Biosens. Bioelectron.*, 2017, **92**, 434–441.

- 18 J. Wan, X. Yan, J. Ding and R. Ren, *Sensors Actuators, B Chem.*, 2010, **146**, 221–225.
- 19 X. Wu, H. Jiang, Y. Zhou, J. Li, C. Wu, C. Wu, B. Chen and X. Wang, *Electrochem. commun.*, 2010, **12**, 962–965.
- 20 M. Gu, J. Zhang, Y. Li, L. Jiang and J. J. Zhu, *Talanta*, 2009, **80**, 246–249.